

# CONFIGURABLE FIELD MAGNETS FOR A PROTON BEAM DYNAMICS R&D RING

S.J. Brooks\*, RAL, Chilton, OX11 0QX, UK

## Abstract

Magnets with many independently-powered coils can provide nearly arbitrary combinations of multipoles up to a certain order. This paper gives examples of field quality in such an “omni-magnet”, which is normal-conducting and simulated with Poisson. Since the magnets also have quite large apertures they may be used to make a general-purpose FFAG and synchrotron test ring for beam dynamics studies. This could use the 3 MeV  $H^-$  beam from the RAL proton Front End Test Stand (FETS) and outline ring parameters are given for that situation.

## EXTENDING FETS WITH A RING

‘Electron models’ of new accelerators, scaled down in energy and size, are sometimes built first as a way to cheaply verify the beam dynamics. The electron beams can have similar optics [1] and even similar levels of space charge [2] to the real machine. However, a critical stage of many high-intensity proton accelerators is the  $H^-$  stripping injection from the linac into the first ring, where a foil turns  $H^-$  into  $H^+$  and the sign change allows many turns to be stacked without the emittance growing additively. This is an operation electrons cannot simulate but is quite important from a beam dynamics point of view.

To make a model of  $H^-$  injection with the associated issues of space charge and painting, one needs a source of strippable ions at low energy with enough current to have significant space charge. The Front End Test Stand (FETS) [3], currently under construction at RAL, will produce 3 MeV  $H^-$  with  $\sim 50$  mA average current during pulses repeating at 50 Hz. The design also includes a beam chopper to remove beam not fitting in the RF buckets of the ring, another important injection issue at high intensity. Thus FETS is a promising injector for this purpose and it may be possible to build a ring of up to  $\sim 10$  m diameter in an adjacent building in the future. The main technical issue is to determine if a practical stripping system can be built at the low energy of 3 MeV.

## Motivation for Configurable Ring

Both synchrotrons and FFAGs are being considered as options for future high-power proton accelerators, with each of these having many possible lattice structures. It would therefore be useful if during the R&D stage the test ring optics could be configurable, saving the expense of building multiple rings. It is suggested this could be achieved using the configurable magnets presented later in this paper. Such an “omni-ring” would also allow a com-

prehensive test of space charge effects in FFAGs, which is a topic of current interest.

## Outline Omni-Ring Parameters

The overall parameters of the omni-ring are given in table 1, at the injection energy before RF is applied. For comparison, EMMA [1] is 5.274 m in diameter but stores electrons of momentum only 10–20 MeV/c; the proton mass requires much stronger magnets at a given energy.

Table 1: Parameters of the Proton Omni-Ring

Beam energy	3	MeV
Beam momentum	75.09	MeV/c
Magnet packing factor	40	%
Mean dipole in magnet	0.2	T
Ring diameter	6.262	m
Revolution frequency	1.216	MHz
<b>Example cell structure</b>		
Magnets per ring	24	
Cell length	0.8197	m
Magnet length	0.3279	m
Drift length	0.4918	m

The injection line from FETS to the ring would ideally contain programmable kickers for injection painting in multiple axes, possibly with RF too. A fast extraction line should be equipped with diagnostics to accurately map the beam profile and halo after various numbers of turns.

## OMNI-MAGNET

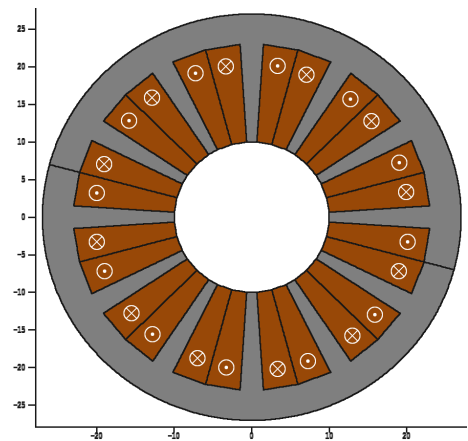


Figure 1: Cross-section of the omni-magnet. The reference current direction shown may be reversed in operation.

\* stephen.brooks@stfc.ac.uk

As shown in figure 1, the magnet resembles a dodecapole but the current in the coil surrounding each iron pole can be varied independently. The bore radius is 10 cm, surrounded by 13 cm-long poles and a 4 cm-thick iron return yoke for a total radius of 27 cm. The poles take up 25% of the angular fraction, the rest being split equally between the conducting coils. This geometry can produce up to a 0.2416 T main dipole field using a maximum current density of 5 A/mm<sup>2</sup>.

### Multipole Fields

Multipole fields can be generated by giving the coil in direction  $(x, y) = (\cos \theta, \sin \theta)$  the current density  $j_{n,\theta} = j_{\max} \sin(n\theta)/n$ , where  $n = 1, 2, \dots$  correspond to dipole, quadrupole etc. and  $j_{\max} = 5 \text{ A/mm}^2$  for this magnet. The division by  $n$  is necessary to avoid saturation, otherwise the fluxes in the poles increase for higher  $n$ . The resulting fields are given in figure 2, from Poisson simulations with a 2 mm mesh size. Table 2 gives the best fit multipole strengths produced.

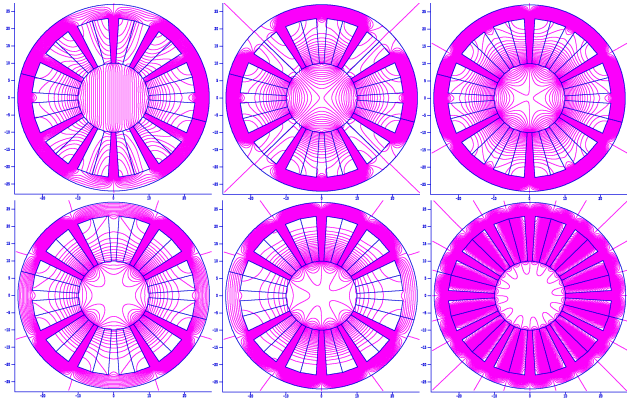


Figure 2: Dipole up to decapole fields. The sixth plot is a “monopole” current configuration where the field cancels.

$n$	Pole	Max $j$ A/mm <sup>2</sup>	Strength T/m <sup><math>n-1</math></sup>	Max $B$ in poles Tesla
1	Dipole	5	0.241558	1.23
2	Quad	2.165	2.21262	1.13
3	Sext	1.667	39.36	1.37
4	Oct	1.083	1032	1.20
5	Deca	1	34800	1.30

$n$	Skew	Max $j$	Strength	Max $B$ in poles
1	Dipole	5	0.241558	1.23
2	Quad	2.5	2.21136	1.29
3	Sext	1.667	39.38	1.37
4	Oct	1.25	1032	1.38
5	Deca	1	34800	1.30
6	Dodeca	0.833	2892000	1.15

Relative field error is defined as  $|\mathbf{B} - \mathbf{B}^*|/|\mathbf{B}^*|$  at each point, where  $\mathbf{B}^*$  is the ideal field. The field errors for the

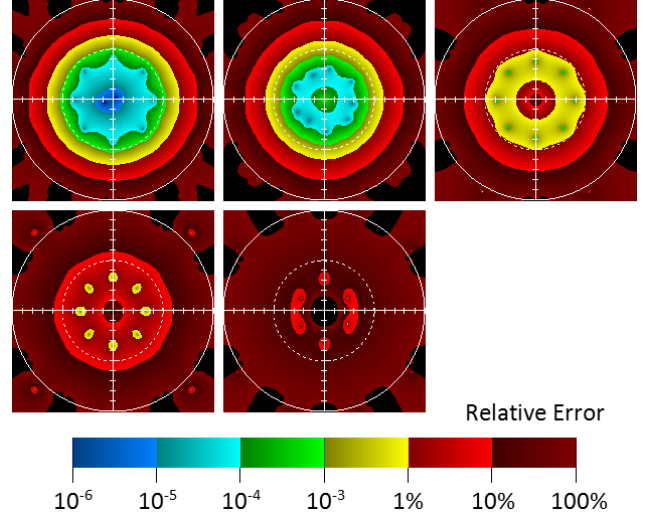


Figure 3: Relative errors of the multipole fields, with the colour scale used throughout this paper. Each plot shows  $-10 \leq x, y \leq 10 \text{ cm}$ , including the entire magnet bore.

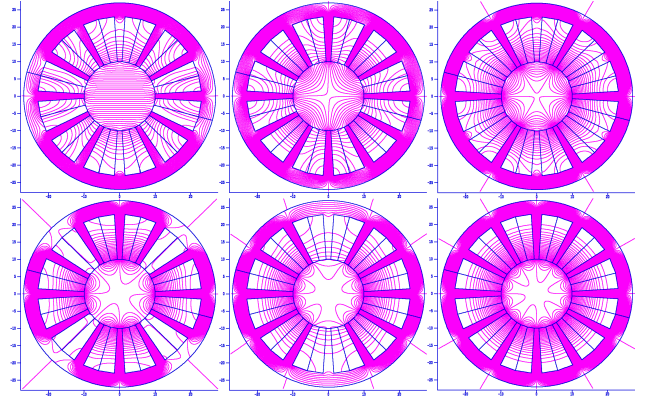


Figure 4: Skew multipole fields from dipole to dodecapole.

normal poles are plotted in figure 3. Skew poles are generated using the currents  $j_{n,\theta}^{\text{skew}} = j_{\max} \cos(n\theta)/n$  and are shown in figure 4, with errors plotted in figure 5. The 12 independent coils should theoretically produce 12 Fourier modes; six of these are skew and five are normal multipoles, with the remaining zero-frequency mode shown in figure 2 producing field cancellation and a weak 24-pole where the flux returns through the copper windings.

### Scaling FFAG Fields

Linear combinations of the multipole current configurations above should be able to approximate any field up to decapole order. Magnets in scaling FFAGs [4] have a field on the  $y = 0$  plane of  $B_y = B_0(r/R_0)^k$ , where  $r = R_0 + x$  is the distance from the ring centre. In this example, the machine radius  $R_0 = 3.131 \text{ m}$  and the scaling index  $k = 20$  is chosen. For a central field strength of  $B_0 = 0.2 \text{ T}$ , the magnet generates the field shown in figure 6. The field accuracy varies depending on the field strength required, with errors shown in figure 7.

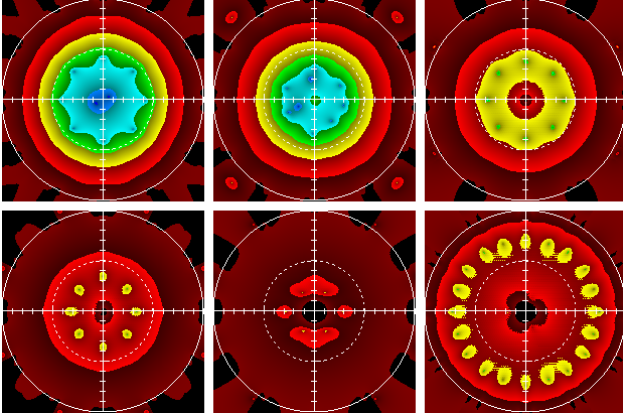


Figure 5: Relative errors of the skew multipole fields.

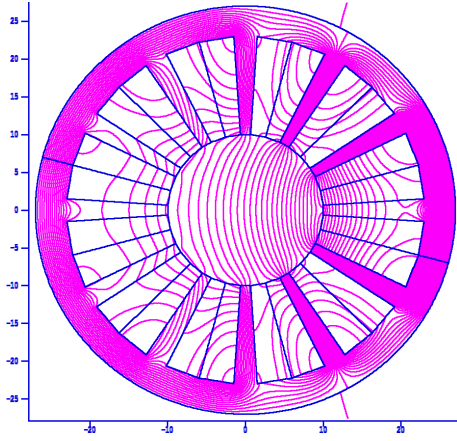


Figure 6: Omni-magnet producing a scaling FFAG field with  $k = 20$ .

### Exponential VFFAG Field

Magnets in vertical orbit excursion FFAGs (VFFAGs) [5] have a field that varies exponentially on the vertical axis:  $B_y = B_0 e^{ky}$  for  $x = 0$ . The fields generated for  $k = 5$  and  $10 \text{ m}^{-1}$  are shown in figure 8 and the errors for various central field strengths in figure 9.

### FUTURE WORK

So far the current densities for each multipole have been determined directly from a formula and therefore may benefit from some correction: the higher poles have a small dipole defect in the simulations for example, which could be subtracted out with a small admixture of  $j_{1,\theta}$ . A simi-

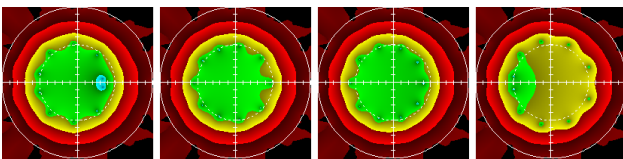


Figure 7: Relative field errors in the  $k = 20$  scaling FFAG for  $B_0 = 0.05, 0.1, 0.15$  and  $0.2 \text{ T}$  (left to right).

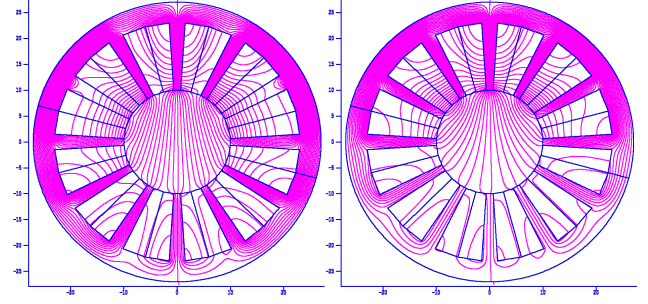


Figure 8: Omni-magnet producing exponential VFFAG fields with  $k = 5 \text{ m}^{-1}$  (left) and  $k = 10 \text{ m}^{-1}$  (right).

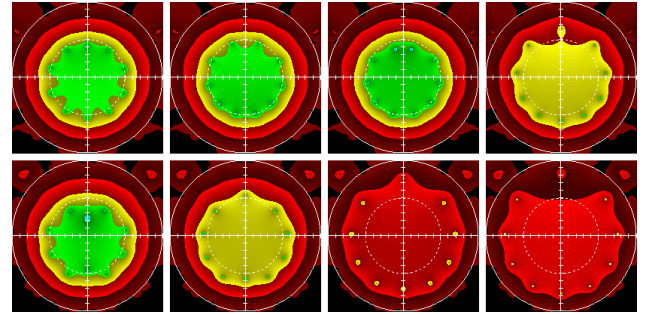


Figure 9: Relative field errors in VFFAG fields with  $k = 5 \text{ m}^{-1}$  (top) and  $k = 10 \text{ m}^{-1}$  (bottom), for  $B_0 = 0.05, 0.1, 0.15$  and  $0.2 \text{ T}$  (left to right).

lar correction scheme would also be used in reality when calibrating each physical magnet.

The saturation of the iron poles stems from the fact they only take up 25% of the circumference of the magnet bore, meaning if the iron starts to saturate at  $1.4 \text{ T}$ , the maximum nominal field at the edge of the bore should only be 25% of this ( $0.35 \text{ T}$ ) since all the flux lines have to bunch together and go through the iron.

Finally, it should be noted the corrector magnets in the SRS designed by Neil Marks [6] have a very similar design and principle to omni-magnets but operate at lower fields. They also have the interesting feature of windings around the iron return yoke rather than the poles, which may mean less current is required for the low-order multipoles.

### REFERENCES

- [1] *Acceleration in the linear non-scaling fixed-field alternating-gradient accelerator EMMA*, S. Machida *et al.*, Nature Physics **8**, pp.243–247 (2012).
- [2] *The University of Maryland Electron Ring (UMER)*, P.G. O’Shea *et al.*, Proc. PAC2001.
- [3] *The RAL Front End Test Stand*, A.P. Letchford *et al.*, Proc. EPAC2006.
- [4] K.R. Symon, *The FFAG Synchrotron—Mark I*, MURA note 043 (1954).
- [5] *Vertical Orbit Excursion FFAGs*, S.J. Brooks, Proc. HB2010.
- [6] *The Operation of Multipole Magnets in the SRS*, R.P. Walker, Proc. PAC1981.